



---

Year: 2020

---

## Highly Efficient Green Solution Processable Organic Light-Emitting Diodes Based on a Phosphorescent 3-(N<sup>CC</sup>)Gold(III) – Alkynyl Complex

Beucher, Hélène ; Kumar, Sudhir ; Merino, Estíbaliz ; Hu, Wei-Hsu ; Stemmler, Gerrit ;  
Cuesta-Galisteo, Sergio ; González, Jorge A ; Jagielski, Jakub ; Shih, Chih-Jen ; Nevado, Cristina

Abstract: Gold(III) complexes are emerging as promising phosphorescent emitters for high-efficiency organic light-emitting diodes (OLEDs). However, despite recent advances in the coordination and organometallic chemistry of gold, only few compounds have been successful in high-performance devices. Here, we disclose the synthesis of a new phosphorescent 3-(N<sup>CC</sup>) – aminophenylalkynyl – N, N – bisfluorenyl – Au(III) complex which exhibits a current efficiency (CE) of 56.4 cd/A and an external quantum efficiency (EQE) of 11.2%. This complex shows a remarkable electroluminescent performance for potential application in highly efficient OLEDs.

DOI: <https://doi.org/10.1021/acs.chemmater.9b04990>

Posted at the Zurich Open Repository and Archive, University of Zurich

ZORA URL: <https://doi.org/10.5167/uzh-188796>

Journal Article

Accepted Version

Originally published at:

Beucher, Hélène; Kumar, Sudhir; Merino, Estíbaliz; Hu, Wei-Hsu; Stemmler, Gerrit; Cuesta-Galisteo, Sergio; González, Jorge A; Jagielski, Jakub; Shih, Chih-Jen; Nevado, Cristina (2020). Highly Efficient Green Solution Processable Organic Light-Emitting Diodes Based on a Phosphorescent 3-(N<sup>CC</sup>)Gold(III) – Alkynyl Complex. *Chemistry of Materials*, 32(4) : 1605 – 1611.

DOI: <https://doi.org/10.1021/acs.chemmater.9b04990>

# Highly Efficient Green Solution Processable OLEDs Based on a Phosphorescent $\kappa^3$ -(N<sup>^</sup>C<sup>^</sup>C)Gold(III)-Alkynyl Complex

Hélène Beucher,<sup>‡§</sup> Sudhir Kumar,<sup>†§</sup> Estíbaliz Merino,<sup>‡r</sup> Wei-Hsu Hu,<sup>†</sup> Gerrit Stemmler,<sup>†</sup> Sergio Cuesta-Galisteo,<sup>‡</sup> Jorge A. González,<sup>‡</sup> Jakub Jagielski,<sup>†</sup> Chih-Jen Shih,<sup>†\*</sup> and Cristina Nevado<sup>‡\*</sup>

<sup>‡</sup>Department of Chemistry, University of Zurich, Winterthurerstrasse 190, CH-8057, Zürich, Switzerland.

<sup>†</sup>Institute for Chemical and Bioengineering, Department of Chemistry and Applied Biosciences, ETH-Zurich, CH-8093, Zürich, Switzerland

**ABSTRACT:** Gold(III) complexes are emerging as promising phosphorescent emitters for high-efficiency OLEDs. However, despite recent advances in the coordination and organometallic chemistry of gold, only few compounds have been successful in high-performance devices. Here, we disclose the synthesis of a new phosphorescent  $\kappa^3$ -(N<sup>^</sup>C<sup>^</sup>C)-aminophenylalkynyl-*N,N'*-bisfluorenyl-Au(III) complex which exhibits a current efficiency ( $\eta_{CE}$ ) of 56.4 cd A<sup>-1</sup> and an external quantum efficiency ( $\eta_{ext}$ ) of 16.2% in solution processable OLED devices. Our findings establish a new branch of gold(III)-alkyne compounds with remarkable electroluminescent performance for potential application in highly-efficient OLEDs.

Phosphorescent emitters have emerged as promising candidates for high-efficiency organic light-emitting diodes (OLEDs).<sup>1,2</sup> These compounds enable to harvest both triplet and singlet excitations, boosting the theoretical limit of the internal quantum efficiency in device to nearly 100%. The heavy metal-induced spin-orbit coupling is responsible for the efficient intersystem crossing, such that the emission comes from the low-energy, quantum-mechanically forbidden triplet states.<sup>3-5</sup> In addition to the complexes derived from iridium(III),<sup>6-13</sup> platinum(II),<sup>14-19</sup> ruthenium(III)<sup>20-22</sup> and osmium(II),<sup>22-24</sup> that have shown promising electroluminescent (EL) characteristics, gold(III) analogs, mostly based on the classical  $\kappa^3$ -(C<sup>^</sup>N<sup>^</sup>C) pincer ligands (with N = pyridine or pyrazine), have recently attracted a lot of attention owing to gold's natural abundance and innate stability.<sup>25-44</sup> Nevertheless, due to the low-lying d-d state and high electrophilicity, only few gold(III) complexes have been explored in the OLED-fabrication context.<sup>25-34</sup> In these compounds though, the unfavorable ligand-to-metal charge transfer transitions (LMCT) [ $\sigma(\text{ligand}) \rightarrow d\sigma^*(\text{metal})$ ] often cause non-radiative losses.<sup>45</sup>

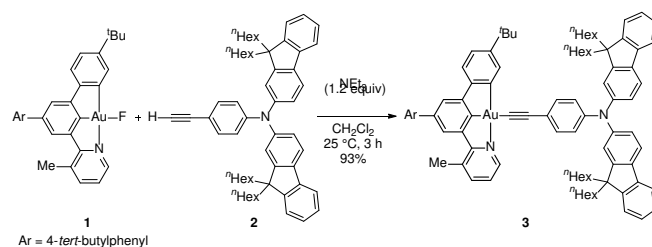
Aiming to characterize highly reactive gold(III) intermediates proposed in oxidative cross-coupling reactions,<sup>46-51</sup> our group synthesized, for the first time, a new family of  $\kappa^3$ -(N<sup>^</sup>C<sup>^</sup>C)Au(III) complexes. The strong  $\sigma$ -donor character of the central anionic Csp<sup>2</sup>-ligand enabled the successful isolation of previously elusive gold(III)-fluoride,<sup>52</sup> formate<sup>53</sup> and carboxylate<sup>54</sup> systems. Further, the  $\kappa^3$ -(N<sup>^</sup>C<sup>^</sup>C) ligand template increased the energy barrier between the triplet and the singlet non-emissive excited states presumably reducing the non-radiative losses. As such, and in contrast to the classical  $\kappa^3$ -(C<sup>^</sup>N<sup>^</sup>C)Au(III)Cl pincer complexes, which are barely emissive in solution at room temperature, the  $\kappa^3$ -(N<sup>^</sup>C<sup>^</sup>C)Au(III)-Cl, -F and -alkynyl derivatives prepared in our

group showed remarkable photoluminescence (PL) at 25 °C in solution, with PLQYs up to 28%.<sup>52</sup> Recently, a high-performance OLEDs based on a carbazole derivative of this template has also been recently described.<sup>55</sup>

Encouraged by these promising results, we report here a strongly luminescent  $\kappa^3$ -(N<sup>^</sup>C<sup>^</sup>C)-aminophenylalkynyl-*N,N'*-bisfluorenyl-Au(III) complex **3**, which has been successfully utilized for the construction of green solution-processable OLEDs. The resulting devices display remarkable performance with EQEs of up to 16.2% and maximum current ( $\eta_{CE}$ ) and power efficiency ( $\eta_{PE}$ ) of 56.4 cd A<sup>-1</sup> and 50.6 lm W<sup>-1</sup>, respectively. These results contrast with recent observations by Yam et al. regarding the instability of related alkynyl complexes,<sup>55</sup> thus highlighting how the careful combination of robust ancillary and anionic ligands can result in high-performance  $\kappa^3$ -(N<sup>^</sup>C<sup>^</sup>C)-Au(III)-alkynyl based OLEDs.

The synthesis of complex **3** is shown in Scheme 1.<sup>56</sup> A facile anionic ligand exchange reaction between fluoride precursor **1** with alkyne **2** in the presence of triethylamine in dichloromethane (CH<sub>2</sub>Cl<sub>2</sub>) at 25 °C delivered complex **3** in almost quantitative yield. Complex **3** was stable enough to be isolated by column chromatography on silica gel as a yellow solid and its structure could be unambiguously characterized by both <sup>1</sup>H, <sup>13</sup>C-NMR spectroscopy as well as high-resolution mass spectrometry.<sup>56</sup>

**Scheme 1.** Straightforward preparation of complex **3**.



Studies to characterize the photophysical properties of **3** were carried out in a degassed solution in tetrahydrofuran (THF) at 298 K.<sup>56</sup> The absorption (Abs) spectrum (Figure 1a, black curve) reveals two major feature peaks corresponding to the spin allowed intraligand (IL) [ $\pi(\text{alkyne}) \rightarrow \pi^*(\text{alkyne})$ ] transition at 250–306 nm and to the gold(III) centered IL [ $\pi(\text{N}^{\wedge}\text{C}^{\wedge}\text{C}) \rightarrow \pi^*(\text{N}^{\wedge}\text{C}^{\wedge}\text{C})$ ] transition at 348–405 nm. A relatively weak tail peak beyond 414 nm is proposed to reflect the ligand-to-ligand charge transfer (LLCT) [ $\pi(\text{alkyne}) \rightarrow \pi^*(\text{N}^{\wedge}\text{C}^{\wedge}\text{C})$ ] transition. An optical energy bandgap ( $E_g$ ) of 3.02 eV was determined from the absorption edge. The photoluminescence (PL) spectrum (Figure 1a, red trace), characterized

with the excitation wavelength ( $\lambda_{ex}$ ) of 365 nm, exhibits a structureless emission profile peaking at 572 nm. The PL spectrum is assigned to the combination of the  ${}^3\text{LLCT } \pi[\text{alkyne}] \rightarrow \pi^*[(\text{N}^{\wedge}\text{C}^{\wedge}\text{C})]$  and metal perturbed  ${}^3\text{IL } \pi \rightarrow \pi^*$  transitions of the cyclometalated ligand, in line with density functional theory (DFT) and time-dependent-density function (TDDFT) calculations discussed in the computational section below. The absolute PL quantum efficiencies ( $\eta_{PL}$ ) at 25 °C were determined to be 12.1% and 21.4% in degassed  $\text{CH}_2\text{Cl}_2$  and THF solutions, respectively. Interestingly, a strong positive solvatochromic effect is observed upon increasing the solvent dipole moment, from xylene (0.33 D) to toluene (0.45 D), and THF (1.63 D),<sup>57</sup> owing to the LLCT from the alkynyl triarylamine to the  $\kappa^3\text{-(N}^{\wedge}\text{C}^{\wedge}\text{C)}$  pincer ligand. Indeed, by increasing the polarity of solvent, the formation of more stable excited states tends to induce red-shift emission and peak broadening<sup>58</sup> (For PL spectra of  $10^{-5}$  M solutions of complex **3** in different solvents and additional explanations, see Figure S1 in the Supporting Information).<sup>56</sup>

Additionally, the phosphorescent (Phos) features of complex **3** were determined at 77 K in a nitrogen degassed glassy solution of 2-methyltetrahydrofuran (2-MeTHF) (Figure 1a, blue trace). Compared to the PL spectrum, the Phos emission is more narrowband and blue-shifted, with two vibrational components at 491 and 522 nm, presumably corresponding to the metal perturbed  ${}^3\text{IL}$  transition of the  $(\text{N}^{\wedge}\text{C}^{\wedge}\text{C})$  ligand.<sup>59</sup> The triplet energy ( $E_T$ ), estimated from the emission maxima in the Phos spectrum, resulted in a value of 2.53 eV. The time-resolved (TR) PL response was simultaneously characterized (Figure S4 and S5 in the SI). At 298 K, the PL decay displays the prompt component with a lifetime  $\tau_1$  of 2.7 ns and the delayed component with a lifetime  $\tau_2$  of 144.2 ns (Figure S4). At 77 K, the Phos decay becomes mono-exponential with a long lifetime  $\tau$  of 45.1  $\mu\text{s}$  (Figure S5). The observed long lifetime at 77 K is a clear signature for a phosphorescent compound.<sup>59,60</sup>

The electrochemical behavior of complex **3** was characterized using cyclic voltammetry (CV) (Figure 1b).<sup>56</sup> An irreversible reduction potential wave emerges at -1.63 V, which is attributed to the cyclometalated  $\kappa^3\text{-(N}^{\wedge}\text{C}^{\wedge}\text{C)}$  ligand.<sup>29,32,38,55</sup> The first irreversible oxidation potential curve at +0.76 V is assigned to the alkyne unit of triarylamine ligand.<sup>26,29,32</sup> Moreover, a secondary quasi-reversible oxidation couple at +0.86 V could be associated to the fluorene subunits of the ancillary ligand itself.<sup>29</sup> The energy levels of the highest occupied molecular orbital (HOMO) and the lowest unoccupied molecular orbital (LUMO) of **3** were therefore determined to be -5.56 eV and -2.54 eV, respectively (Table S1 in the SI).

Differential scanning calorimetry (DSC) and thermogravimetric analysis (TGA) were used to study the thermal properties of this new complex.<sup>56</sup> A high thermal stability was observed, with a decomposition temperature ( $T_d$ ) of 337 °C and a glass transition ( $T_g$ ) temperature of 146 °C (Figures S2 and S3 in the SI). We attribute these remarkable features to the rigid nature of the fluorene and acetylenic groups as well as to the strong  $\pi \rightarrow \pi^*$  interactions between the pincer and the alkynyl ligand.<sup>61,62</sup> Note that a high  $T_g$  is prerequisite for forming intact amorphous films in OLEDs.

DFT and TDDFT calculations were carried out to gain a deeper understanding of the electronic structure and the origin of the electronic transitions observed for this compound.<sup>56</sup> Its optimized ground-state ( $S_0$ ) geometry including selected structural parameters is shown in Figure 2a. Calculations of the first ten singlet-singlet transitions in **3** and the frontier orbitals involved in these transitions can be found in Table S4 and in Figure S13 in the Supporting Information, respectively. The analysis of the transitions with a large coefficient and non-zero significant oscillator strengths in the region of the low-lying absorption bands for complex **3** (ca. 459 nm) correlate with major contributions from the HOMO  $\rightarrow$  LUMO

and HOMO  $\rightarrow$  LUMO+2 excitations. The HOMO is predominantly the  $\pi$  orbital of the ethynyltriphenylamine ligand. The LUMO correlates with the  $\pi^*$  orbital of the pyridine moiety and the central aromatic ring of the pincer ligand whereas the LUMO+2 correlates with the  $\pi^*$  orbitals of the fluorene moieties. Thus, the low-lying absorption bands measured for **3** can be assigned to the metal-perturbed LLCT [ $\pi(\text{alkyne}) \rightarrow \pi^*(\text{N}^{\wedge}\text{C}^{\wedge}\text{C})$ ] and the IL [ $\pi(\text{alkyne}) \rightarrow \pi^*(\text{alkyne})$ ] transitions (vide supra). The energy gap between HOMO-LUMO orbitals is computed to be 3.10 eV, in good agreement with the experimental results obtained from the CV experiments. Optimization of the geometry of the lowest-lying triplet excited state ( $T_1$ ) has been performed to provide further insights into the nature of the emissive states of **3**. Differences in bond lengths between the  $T_1$  states and the corresponding ground states are shown in Figure S14 in the Supporting Information although no major geometrical changes were found and the geometry in both its  $S_0$  and  $T_1$  states is maintained so that no major excited state structure distortions were observed. The plots of the spin density of the emissive state are mainly localized on both the pincer and the alkynyl ligand as well as on the metal center, supporting a mixture of metal-perturbed  ${}^3\text{IL}$  and  ${}^3\text{LLCT}$  character in the  $T_1$  state (Figure 2b). The calculated emission energy of **3** is 522 nm, which is relatively close to the results disclosed in the PL spectrum and explains the green emission observed for this complex.

**Table 1.** Photophysical characteristics of complex **3**.

$\lambda_{\text{Abs}}$ (nm)	$\epsilon$ (L.mol <sup>-1</sup> .cm <sup>-1</sup> )	$\lambda_{\text{PL}}$ (nm)	$\lambda_{\text{Phos}}$ (nm)	$\phi_{\text{QY}}$ (%)
273, 359	42215, 33869	572	491, 522	21.4

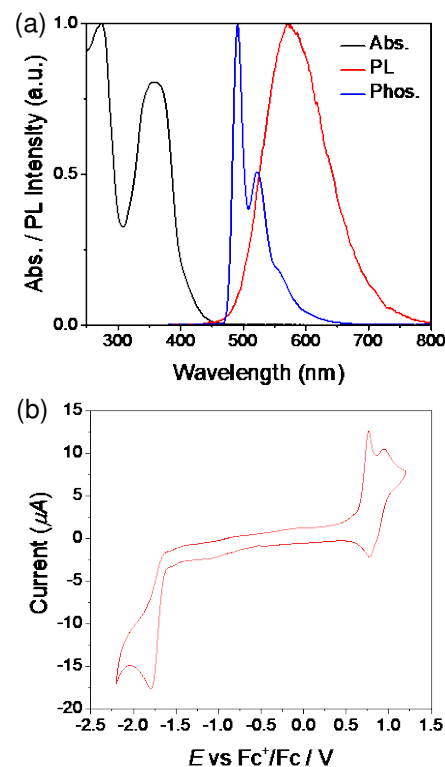


**Figure 1.** (a) Absorbance (Abs) in black (in THF at 298 K), photoluminescence (PL) spectra in red (in 2-MeTHF at 298 K) and phosphorescence (Phos) spectra in blue (in 2-MeTHF at 77 K) of **3**. (b) Cyclic voltammogram of **3** recorded in argon-degassed  $\text{CH}_2\text{Cl}_2$  with a 0.1 M tetrabutylammonium hexafluorophosphate (TBAHFP) electrolyte, an internal reference of ferrocene and a glassy carbon working electrode.

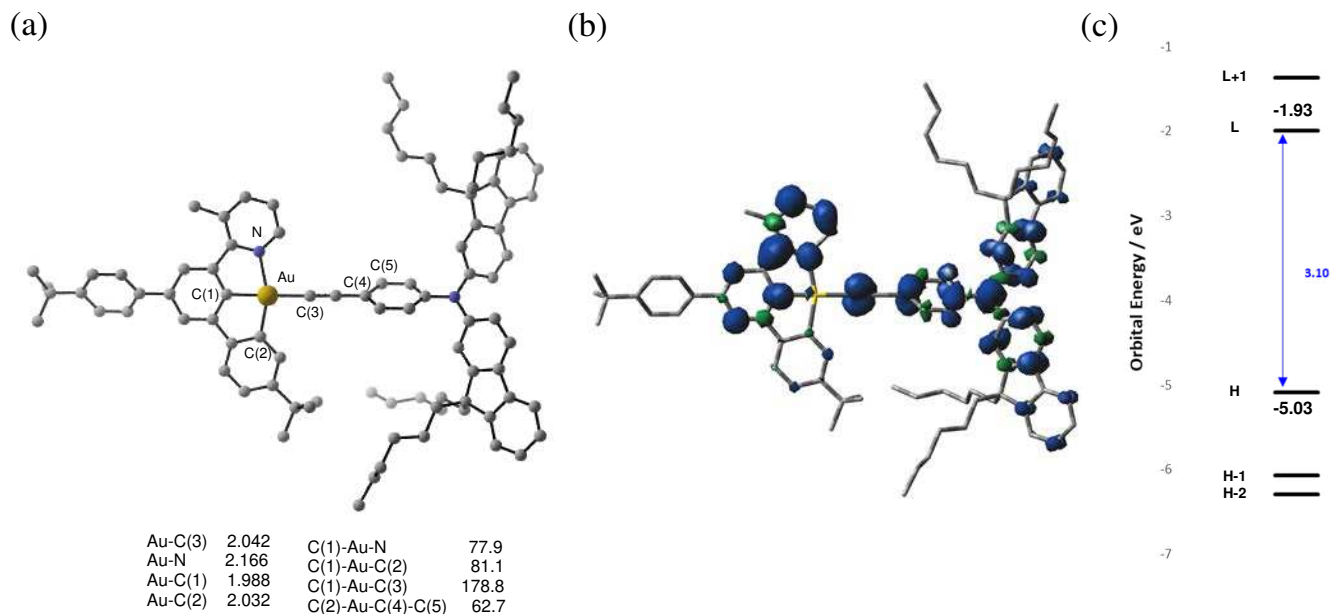


**Figure 2.** (a) Optimized ground-state geometry of **3**. H atoms are omitted for clarity. Bond distances are given in Angstroms ( $\text{\AA}$ ) and angles in degrees ( $^\circ$ ). (b) Plot of the spin density (isovalue = 0.002) of the emissive state of **3**. H atoms are omitted for clarity. (c) Orbital energy diagram of the frontier molecular orbitals of **3**.

To evaluate the electroluminescence (EL) characteristics of complex **3**, solution-processed emission layer (EML) was used in OLED devices. At the outset, the EML was prepared by varying the doping concentration of complex **3** from 5 to 20 wt% in five different hosts, 4,4'-bis-(*N*-carbazolyl)-1,1'-biphenyl (CBP), poly(9-vinylcarbazole) (PVK), 2,6-bis-(3-(9*H*-carbazol-9-yl)phenyl)pyridine (26DCzPPy), bis-4-(*N*-carbazolyl)-phenylphenylphosphine oxide (BCPO) and PVK: 1,3-bis[2-(4-*tert*-butylphenyl)-1,3,4-oxadiazol-5-yl]benzene (OXD-7) mixed host with a respective ratio of 60:40 (see Figure S7 in the Supporting Information). A device architecture of indium tin oxide (ITO; 120 nm) anode/poly(3,4-ethylene-dioxythiophene)-poly(styrene sulfonate) (PEDOT:PSS;  $32 \pm 3$  nm)/EML ( $32 \pm 1$  nm)/2,2',2''-(1,3,5-benzinetriyl)-tris(1-phenyl-1-*H*-benzimidazole) (TPBI; 35 nm)/lithium fluoride (LiF; 1 nm)/aluminum (Al; 100 nm) cathode was selected for subsequent studies (Figure S6a).

Numerous devices were fabricated to optimize the host matrix and emitter doping concentration (See summary in Table S2 and Figure S8 in the Supporting Information). The device based on PVK:OXD-7 (60:40) mixed host and 10 wt% complex **3** showed the best performance among all five hosts studied with a maximum  $\eta_{CE}$  of  $46.6 \text{ cd A}^{-1}$  and  $\eta_{ext}$  of 14.1%. Moreover, complex **3** shows a high  $\eta_{PL}$  of  $68 \pm 5\%$  by doping with the PVK:OXD-7 (60:40) mixed host matrix. The EL spectrum exhibits the maximum at 508 nm together with a power efficiency ( $\eta_{PE}$ ) of  $32.6 \text{ lm W}^{-1}$ . The high efficiencies in the PVK:OXD-7 mixed host device is attributed to the following factors: (i) The host-to-guest energy transfer is efficient due to a large overlap of host emission and guest absorbance spectra (Figure S9). (ii) The mixed host design enables effective carrier injection as PVK has a shallow HOMO energy (-5.8 eV; for hole injection) and OXD-7 has a lower LUMO compared to ETL (-0.3 eV; for electron injection).<sup>61</sup> (iii) The angle-dependent PL measurement reveals that the emission dipole is moderately oriented horizontally, having the probability of in-plane dipole of 68%, which slightly increases the light outcoupling efficiency (Table S3 and Figure S10 in the Supporting Information). As shown in Figure S8n and Table S2, the EL

emission maximum gradually redshifts from 504 to 524 nm and CIE<sub>x,y</sub> coordinates from (0.253, 0.553) to (0.292, 0.583) by increasing the doping concentration from 5 to 20 wt%.

Further optimization led to an even higher  $\eta_{CE}$  ( $\eta_{ext}$  and  $\eta_{PE}$ ) of  $56.4 \text{ cd A}^{-1}$  (16.2% and  $50.6 \text{ lm W}^{-1}$ ) at  $100 \text{ cd m}^{-2}$  by depositing a thin layer of hole transport layer (HTL) of Poly-TPD after PEDOT:PSS layer and a 5 nm thin hole confinement layer of POT2T before TPBi layer (Figure 3 and Figure S7b in Supporting Information). In addition, the TPBi layer thickness was also increased from 35 nm to 45 nm to improve the light-outcoupling by reducing the surface plasmonic loss as affirmed by optical simulations (Figure S11). The device also demonstrates the highest luminance of  $>9000 \text{ cd m}^{-2}$  at the current density of  $113 \text{ mA cm}^{-2}$ . High EL performance and low efficiency roll-off appears to stem from a balanced carrier injection and effective carrier confinement within the emissive layer.<sup>63</sup> As illustrated in Figure S12, the EL emission spectra demonstrate excellent stability throughout the operation voltage ranging from 4 V to 8 V.

In conclusion, we report here a highly efficient green solution processable phosphorescent OLED based on a newly synthesized  $\kappa^3$ -(*N*<sup>^C</sup><sup>^C</sup>)<sup>^C</sup>-aminophenylalkynyl-*N,N'*-bisfluorenyl-Au(III) complex. The device, with a maximum  $\eta_{CE}$  of  $56.4 \text{ cd A}^{-1}$  and  $\eta_{ext}$  of 16.2% represents a new entry towards the development of low-cost solution-processed OLEDs. Further optimization in the structure of the gold(III) complex and in the fabrication of devices is ongoing in our laboratories and will be reported in due course.

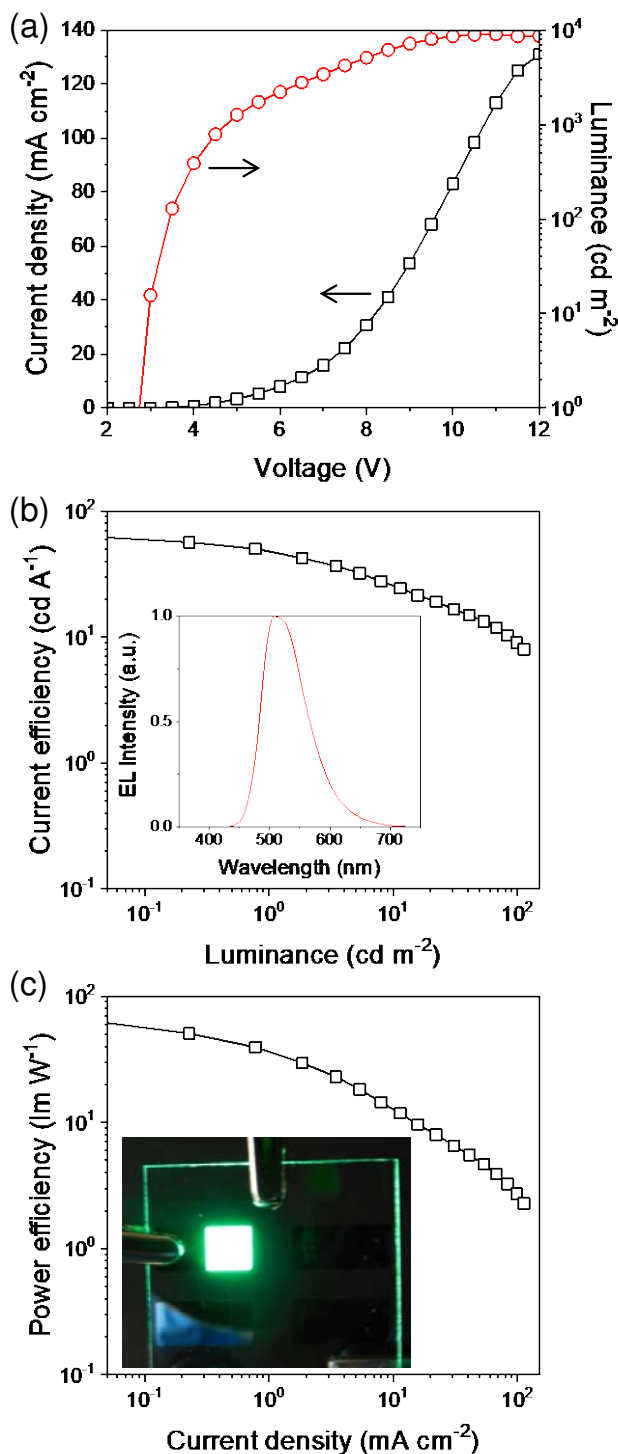


**Figure 3.** EL characteristics of devices containing 10 wt% of **3** in the PVK:OXD-7 (60:40) host. (a) Current density and luminance as a function of voltage. (b) Current efficiency as a function of current density. Inset: EL spectrum of device at 4 V. (c) Power efficiency as a function of current density. Inset: Photograph of an OLED device with an active area of 25 mm<sup>2</sup>.

## EXPERIMENTAL/METHODS

**Synthesis of Materials.** The detailed synthesis and characterization of the newly developed gold(III) complex is described in the Supporting Information.

**Theoretical Calculation.** DFT calculations were performed using Gaussian 09.5.<sup>56</sup>

**Electrochemistry.** CV measurements were carried out on a Metrohm Autolab potentiostat/galvanostat using a platinum wire counter electrode and a glassy carbon working electrode.<sup>56</sup>

**Photophysical Measurements.** Ultraviolet-visible (UV-vis) spectrum of gold(III) complex was collected in 10<sup>-5</sup> M in dichloromethane (DCM) using a JASCO V670 spectrometer. Photoluminescence (PL) spectra were recorded with Hamamatsu CCD spectrometer at an excitation wavelength of 370 nm. Time resolved photoluminescence (TRPL) spectra were collected using a Hamamatsu Quantaaurus-Tau (Q-Tau) Fluorescence Lifetime Spectrometer (C11367-31) equipped with a time correlated single photon counting (TCSPC) measurement system. Phosphorescence spectra were acquired using a Hamamatsu Quantaaurus-Tau (Q-tau) Fluorescence Lifetime Spectrometer (C11367-31) equipped with an OptistatDN2 cryostat from Oxford Instruments.<sup>56</sup>

**Device Fabrication and Characterization.** Patterned ITO coated glass substrates were brush cleaned using the Extran MA02 neutral detergent and deionized (DI) water mixture (1:3). Subsequently, all substrates were sequentially sonicated in acetone and isopropanol, each 20 min., then irradiated in oxygen plasma for 10 min. Thereafter, an aqueous PEDOT:PSS solution was spin-coated at a speed of 4000 rpm for 50 s then annealed at 130 °C for 30 min. in the ambient conditions. These substrates were then transferred into a nitrogen filled glovebox for the deposition of successive layers. An optional hole transporting layer (HTL) of Poly-TPD was spin-coated on PEDOT:PSS layer at 3000 rpm for 40 s then annealed at 130 °C for 30 min. Successively, the emission layers (EML) were spin-casted at 2500 rpm for 40 s, which comprised the mixture of complex and host (polymeric or molecular). All substrates were transferred in the ultrahigh vacuum chamber (~8×10<sup>-8</sup> mbar). Subsequently, an optimized ETL (TPBi), hole blocking layer (PO-T2T), and EIL (LiF) was thermally evaporated on the EML through thermal evaporation. Finally, a 100 nm Al cathode layer was also deposited on the EIL through a shadow mask. Each substrate is designed to realize four pixels, each with an active area of 25 mm<sup>2</sup> as defined by the overlapping between Al and ITO layers. All the devices were stored in the glove box and characterized under the ambient conditions.<sup>56</sup>

## ASSOCIATED CONTENT

### Supporting Information

Supplementary information including compound synthesis, characterization, OLED devices fabrication and characterization and DFT calculations. This material is available free of charge via the Internet at <http://pubs.acs.org>.

## AUTHOR INFORMATION

### Corresponding Author

Chih-Jen Shih\* ([chih-jen.shih@chem.ethz.ch](mailto:chih-jen.shih@chem.ethz.ch))  
Cristina Nevado\* ([cristina.nevado@chem.uzh.ch](mailto:cristina.nevado@chem.uzh.ch))

### Present Address

<sup>†</sup>E.M.: Department of Organic and Inorganic Chemistry, Chemical Research Institute Andrés M. del Río (IQAR), University of Alcalá, 28805-Alcalá de Henares (Madrid), Spain.

### Author Contributions

<sup>§</sup>These authors contributed equally.



## Notes

The authors declare no competing financial interests.

## ACKNOWLEDGMENTS

CN thank the European Research Council (ERC Starting grant agreement no. 307948) and the Swiss National Science Foundation (SNF) (200020-146853), for financial support. CJS is grateful for the financial support from SNF (200021-178944) and ETH Zurich. We thank Dr. Reinhard O. Kissner's for the CV measurements and Raphaël Brechbühler for TR-PL measurements at 77 K.

## REFERENCES

- (1) Baldo, M. A.; Thompson, M. E.; Forrest, S. R. High-Efficiency Fluorescent Organic Light-Emitting Devices Using a Phosphorescent Sensitizer. *Nature* **2000**, *403*, 750.
- (2) Bhatnagar, P.K. Organic Light-Emitting Diodes—A Review. In: *Khan Z. (eds) Nanomaterials and Their Applications. Advanced Structured Materials*; Springer, Singapore, **2018**, *84*, 261.
- (3) Baldo, M. A.; O'Brien, D. F.; Thompson, M. E.; Forrest, S. R. Excitonic Singlet-Triplet Ratio in a Semiconducting Organic Thin Film. *Phys. Rev. B* **1999**, *60*, 14422.
- (4) Yersin, H.; Rausch, A. F.; Czerwiec, R.; Hofbeck, T.; Fischre, T. The Triplet State of Organo-Transition Metal Compounds. Triplet Harvesting and Singlet Harvesting for Efficient OLEDs. *Coord. Chem. Rev.* **2011**, *255*, 2622.
- (5) Kleinschmidt, M.; van Müllen, C.; Marian, C. M. Intersystem-Crossing and Phosphorescence Rates in *fac*-Ir<sup>III</sup>(ppy)<sub>3</sub>: A Theoretical Study Involving Multi-Reference Configuration Interaction Wavefunctions. *J. Chem. Phys.* **2015**, *142*, 094301.
- (6) Adachi, C.; Baldo, M. A.; Thompson, M. E.; Forrest, S. R. Nearly 100% Internal Phosphorescence Efficiency in an Organic Light Emitting Device. *J. Appl. Phys.* **2001**, *90*, 5048.
- (7) Lamansky, S.; Djurovic, P.; Murphy, D.; Abdel-Razzaq, F.; Lee, H.-E.; Adachi, C.; Burrows, P. E.; Forrest, S. R.; Thompson, M. E. Highly Phosphorescent Bis-Cyclometalated Iridium Complexes: Synthesis, Photophysical Characterization, and Use in Organic Light Emitting Diodes. *J. Am. Chem. Soc.* **2001**, *123*, 4304.
- (8) D'Andrade, B. W.; Thompson, M. E.; Forrest, S. R. Controlling Exciton Diffusion in Multilayer White Phosphorescent Organic Light Emitting Devices. *Adv. Mater.* **2002**, *14*, 147.
- (9) Ren, X.; Li, J.; Holmes, R. J.; Djurovic, P. I.; Forrest, S. R.; Thompson, M. E. Ultrahigh Energy Gap Hosts in Deep Blue Organic Electrophosphorescent Devices. *Chem. Mater.* **2004**, *16*, 4743.
- (10) Kawamura, Y.; Goushi, K.; Brooks, J.; Brown, J. J.; Sasabe, H.; Adachi, C. 100% Phosphorescence Quantum Efficiency of Ir(III) Complexes in Organic Semiconductor Films. *Appl. Phys. Lett.* **2005**, *86*, 071104.
- (11) Bolink, H. J.; Coronado, E.; Santamaria, S. G.; Sessolo, M.; Evans, N.; Klein, C.; Baranoff, E.; Kalyanasundaram, K.; Graetzel, M.; Nazeeruddin, M. K. Highly Phosphorescent Perfect Green Emitting Iridium(III) Complex for Application in OLEDs. *Chem. Commun.* **2007**, 3276.
- (12) Fu, H.; Cheng, Y.-M.; Chou, P.-T.; Chi, Y. Feeling blue? Blue Phosphors for OLEDs. *Mater. Today* **2011**, *14*, 472.
- (13) Lai, P.-N.; Brysacz, C. H.; Alam, M. K.; Ayoub, N. A.; Gray, T. G.; Bao, J.; Teets, T. S. Highly Efficient Red-Emitting Bis-Cyclometalated Iridium Complexes. *J. Am. Chem. Soc.* **2018**, *140*, 10198.
- (14) Baldo, M. A.; O'Brien, D. F.; You, Y.; Shoustikov, A.; Sibley, S.; Thompson, M. E.; Forrest, S. R. Highly Efficient Phosphorescent Emission from Organic Electroluminescent Devices. *Nature* **1998**, *395*, 151.
- (15) Hissler, M.; McGarrah, J. E.; Connick, W. B.; Geiger, D. K.; Cummings, S. D.; Eisenberg, R. Platinum Dimine Complexes: towards a Molecular Photochemical Device. *Coord. Chem. Rev.* **2000**, *208*, 115.
- (16) McMillin, D. R.; Moore, J. J. Luminescence that Lasts from Pt(trpy)Cl<sup>+</sup> Derivatives (trpy=2,2',6',2"-terpyridine). *Coord. Chem. Rev.* **2002**, *229*, 113.
- (17) Lu, W.; Mi, B.-X.; Chan, M. C. W.; Hui, Z.; Che, C.-M.; Zhu, N.; Lee, S.-T. Light-Emitting Tridentate Cyclometalated Platinum(II) Complexes Containing  $\sigma$ -Alkynyl Auxiliaries: Tuning of Photo- and Electrophosphorescence. *J. Am. Chem. Soc.* **2004**, *126*, 4958.
- (18) Castellano, F. N.; Pomestchenko, I. E.; Shikhova, E.; Hua, F.; Muro, M. L.; Rajapakse, N. Photophysics in Bipyridyl and Terpyridyl Platinum(II) Acetylides. *Coord. Chem. Rev.* **2006**, *250*, 1819.
- (19) Lee, C.; Zaen, R.; Park, K.-M.; Lee, K. H.; Lee, J. Y.; Kang, Y. Blue Phosphorescent Platinum Complexes Based on Tridentate Bipyridine Ligands and Their Application to Organic Light-Emitting Diodes (OLEDs). *Organometallics* **2018**, *37*, 4639.
- (20) Rudmann, H.; Shimada, S.; Rubner, M. F. Solid-State Light-Emitting Devices Based on the Tris-Chelated Ruthenium(II) Complex. 4. High-Efficiency Light-Emitting Devices Based on Derivatives of the Tris(2,2'-bipyridyl) Ruthenium(II) Complex. *J. Am. Chem. Soc.* **2002**, *124*, 4918.
- (21) Welter, S.; Brunner, K.; Hofstra, J. W.; De Cola, L. Electroluminescent Device with Reversible Switching Between Red and Green Emission. *Nature* **2003**, *421*, 54.
- (22) Chou, P.-T.; Chi, Y. Contemporary progresses on neutral, highly emissive Os(II) and Ru(II) complexes. *Chem. Soc. Rev.* **2007**, *36*, 1421.
- (23) Tung, Y.-L.; Wu, P.-C.; Liu, C.-S.; Chi, Y.; Yu, J.-K.; Hu, Y.-H.; Chou, P.-T.; Peng, S.-M.; Lee, G.-H.; Tao, Y.; Carty, A. J.; Shu, C.-F.; Wu, F.-L. Highly Efficient Red Phosphorescent Osmium(II) Complexes for OLED Applications. *Organometallics* **2004**, *23*, 3745.
- (24) Du, B.-S.; Liao, J.-J.; Huang, M.-H.; Lin, C.-H.; Lin, H.-W.; Chi, Y.; Pan, H.-A.; Fan, G.-L.; Wong, K.-T.; Lee, G.-H.; Chou, P.-T. Os(II) Based Green to Red Phosphors: A Great Prospect for Solution-Processed, Highly Efficient Organic Light-Emitting Diodes. *Adv. Funct. Mater.* **2012**, *22*, 3491.
- (25) Au, V. K.-M.; Wong, K. M.-C.; Tsang, D. P.-K.; Chan, M.-Y.; Zhu, N.; Yam, V. W.-W. High-Efficiency Green Organic Light-Emitting Devices Utilizing Phosphorescent Bis-cyclometalated Alkynylgold(III) Complexes. *J. Am. Chem. Soc.* **2010**, *132*, 14273.
- (26) Tang, M.-C.; Tsang, D. P.-K.; Chan, M. M.-Y.; Wong, K. M.-C.; Yam, V. W.-W. Dendritic Luminescent Gold(III) Complexes for Highly Efficient Solution-Processable Organic Light-Emitting Devices. *Angew. Chem. Int. Ed.* **2013**, *52*, 446.
- (27) Tang, M.-C.; Tsang, D. P.-K.; Wong, Y.-C.; Chan, M.-Y.; Wong, K. M.-C.; Yam, V. W.-W. Bipolar Gold(III) Complexes for Solution-Processable Organic Light-Emitting Devices with a Small Efficiency Roll-Off. *J. Am. Chem. Soc.* **2014**, *136*, 17861.
- (28) Cheng, G.; Chan, K. T.; To, W.-P.; Che, C.-M. Color Tunable Organic Light-Emitting Devices with External Quantum Efficiency over 20% Based on Strongly Luminescent Gold(III) Complexes having Long-Lived Emissive Excited States. *Adv. Mater.* **2014**, *26*, 2540.
- (29) Tang, M.-C.; Chan, C. K.-M.; Tsang, D. P.-K.; Wong, Y.-C.; Chan, M. M.-Y.; Wong, K. M.-C.; Yam, V. W.-W. Saturated Red-Light-Emitting Gold(III) Triphenylamine Dendrimers for Solution-Processable Organic Light-Emitting Devices. *Chem. Eur. J.* **2014**, *20*, 15233.
- (30) Tang, M.-C.; Lee, C.-H.; Lai, S.-L.; Ng, M.; Chan, M.-Y.; Yam, V. W.-W. Versatile Design Strategy for Highly Luminescent Vacuum-Evaporable and Solution-Processable Tridentate Gold(III) Complexes with Monoaryl Auxiliary Ligands and Their Applications for Phosphorescent Organic Light Emitting Devices. *J. Am. Chem. Soc.* **2017**, *139*, 9341.
- (31) To, W.-P.; Zhou, D.; Tong, G. S. M.; Cheng, G.; Yang, C.; Che, C.-M. Highly Luminescent Pincer Gold(III) Aryl Emitters: Thermally Activated Delayed Fluorescence and Solution-Processed OLEDs. *Angew. Chem. Int. Ed.* **2017**, *516*, 14036.
- (32) Lee, C.-H.; Tang, M.-C.; Wong, Y.-C.; Chan, M.-Y.; Yam, V. W.-W. Sky-Blue-Emitting Dendritic Alkynylgold(III) Complexes for Solution-Processable Organic Light-Emitting Devices. *J. Am. Chem. Soc.* **2017**, *139*, 10539.
- (33) Tang, M.-C.; Lee, C.-H.; Ng, M.; Wong, Y.-C.; Chan, M.-Y.; Yam, V. W.-W. Highly Emissive Fused Heterocyclic Alkynylgold(III) Complexes for Multiple Color Emission Spanning from Green to Red for Solution-Processable Organic Light-Emitting Devices. *Angew. Chem. Int. Ed.* **2018**, *57*, 5463.
- (34) Lee, C.-H.; Tang, M.-C.; Cheung, W.-L.; Lai, S.-L.; Chan, M.-Y.; Yam, V. W.-W. Highly Luminescent Phosphine Oxide-Containing Bipolar Alkynylgold(III) Complexes for Solution-Processable Organic Light-Emitting Devices with Small Efficiency Roll-offs. *Chem. Sci.* **2018**, *9*, 6228.
- (35) Vogler, A.; Kunkely, H. Photoreactivity of Gold Complexes. *Coord. Chem. Rev.* **2001**, *219-221*, 489.
- (36) Yam, V. W.-W.; Cheng, E. C.-C. Highlights on the Recent Advances in Gold Chemistry—a Photophysical Perspective. *Chem. Soc. Rev.* **2008**, *37*, 1806.
- (37) Kumar, R.; Nevado, C. Cyclometalated Gold(III) Complexes: Synthesis, Reactivity, and Physicochemical Properties. *Angew. Chem. Int. Ed.* **2017**, *56*, 1994.
- (38) Yam, V. W.-W.; Wong, K. M.-C.; Hung, L.-L.; Zhu, N. Luminescent Gold(III) Alkynyl Complexes: Synthesis, Structural Characterization, and Luminescence Properties. *Angew. Chem. Int. Ed.* **2005**, *44*, 3107.

- (39) Wong, K. M. C.; Hung, L.-L.; Lam, W. H.; Zhu, N.; Yam, V. W.-W. A Class of Luminescent Cyclometalated Alkynylgold(III) Complexes: Synthesis, Characterization, and Electrochemical, Photophysical, and Computational Studies of [Au(C<sup>N</sup>^C)(C:CR)] (C<sup>N</sup>^C =  $\kappa^3$ C,N,C Bis-cyclometalated 2,6-Diphenylpyridyl). *J. Am. Chem. Soc.* **2007**, *129*, 4350.
- (40) To, W.-P.; Tong, G. S.-M.; Lu, W.; Ma, C.; Liu, J.; Chow, A. L.-F.; Che, C.-C. Luminescent Organogold(III) Complexes with Long-Lived Triplet Excited States for Light-Induced Oxidative C-H Bond Functionalization and Hydrogen Production. *Angew. Chem. Int. Ed.* **2012**, *516*, 2654.
- (41) To, W.-P.; Chan, K. T.; Tsong, G. S. M.; Ma, G.; Kwok, W.-M.; Guan, X.; Low, K.-H.; Che, C.-M. Strongly Luminescent Gold(III) Complexes with Long-Lived Excited States: High Emission Quantum Yields, Energy Up-Conversion, and Nonlinear Optical Properties. *Angew. Chem. Int. Ed.* **2013**, *52*, 6648.
- (42) Fernandez-Cestau, J.; Bertrand, B.; Blaya, M.; Jones, G. A.; Penfold, T. J.; Bochmann, M. Synthesis and Luminescence Modulation of Pyrazine-Based Gold(III) Pincer Complexes. *Chem. Commun.* **2015**, *51*, 16629.
- (43) Fernandez-Cestau, J.; Bertrand, B.; Pintus, A.; Bochmann, M. Synthesis, Structures, and Properties of Luminescent (C<sup>N</sup>^C)gold(III) Alkyl Complexes: Correlation between Photoemission Energies and C-H Acidity. *Organometallics* **2017**, *36*, 3304.
- (44) Currie, L.; Fernandez-Cestau, J.; Rocchigiani, L.; Bertrand, B.; Lancaster, S. J.; Hughes, D. L.; Duckworth, H.; Jones, S. T. E.; Credgington, D.; Penfold, T. J.; Bochmann, M. Luminescent Gold(III) Thiolates: Supramolecular Interactions Trigger and Control Switchable Photoemissions from Bimolecular Excited States. *Chem. Eur. J.* **2017**, *23*, 105.
- (45) Lam, E. S.-H.; Lam, W. H.; Yam, V. W.-W. A Study on the Effect of Dianionic Tridentate Ligands on the Radiative and Nonradiative Processes for Gold(III) Alkynyl Systems by a Computational Approach. *Inorg. Chem.* **2015**, *54*, 3624.
- (46) Zhang, G.; Peng, Y.; Cui, L.; Zhang, L. Gold-Catalyzed Homogeneous Oxidative Cross-Coupling Reactions. *Angew. Chem. Int. Ed.* **2009**, *48*, 3112.
- (47) Brenzovitch, W. E.; Brazeau, J. F.; Toste, F. D. Gold-Catalyzed Oxidative Coupling Reactions with Aryltrimethylsilanes. *Org. Lett.* **2010**, *12*, 4728.
- (48) Hopkinson, M.; Tessier, A.; Salisbury, A.; Giuffredi, G.; Combettes, L.; Gee, A.; Gouverneur, V. Au<sup>I</sup>/Au<sup>III</sup> Catalysis: An Alternative Approach for C-C Oxidative Coupling. *Chem. Eur. J.* **2011**, *17*, 8248.
- (49) Ball, L. T.; Lloyd-Jones, G. C.; Russell, C. A. Gold-Catalyzed Direct Arylation. *Science* **2012**, *337*, 1644.
- (50) Peng, H.; Xi, Y.; Ronaghi, N.; Dong, B.; Akhmedov, N. G.; Shi, X. Gold-Catalyzed Oxidative Cross-Coupling of Terminal Alkynes: Selective Synthesis of Unsymmetrical 1,3-Diynes. *J. Am. Chem. Soc.* **2014**, *136*, 13174.
- (51) Zeineddine, A.; Estévez, L.; Mallet-Ladeira, S.; Miqueu, K.; Amgoune, A.; Bourissou, D. Rational Development of Catalytic Au(I)/Au(III) Arylation Involving Mild Oxidative Addition of Aryl Halides. *Nature Commun.* **2017**, *8*, 565.
- (52) Kumar, R.; Linden, A.; Nevado, C. Luminescent (N<sup>^</sup>C<sup>^</sup>C) Gold(III) Complexes: Stabilized Gold(III) Fluorides. *Angew. Chem. Int. Ed.* **2015**, *54*, 14287.
- (53) Kumar, R.; Krieger, J.-P.; Gómez-Bengoa, E.; Fox, T.; Linden, A.; Nevado, C. The First Gold(III) Formate: Evidence for  $\beta$ -Hydride Elimination. *Angew. Chem. Int. Ed.* **2017**, *56*, 12862.
- (54) Beucher, H.; Merino, E.; Genoux, A.; Fox, T.; Nevado, C.  $\kappa^3$ -(N<sup>^</sup>C<sup>^</sup>C)Gold(III) Carboxylates: Evidence for Decarbonylation Processes. *Angew. Chem. Int. Ed.* **2019**, *58*, 9064.
- (55) Li, I.-K.; Tang, M.-C.; Lai, S.-L.; Ng, M.; Kwok, W.-K.; Chan, M.-Y.; Yam, V. W.-W. Strategies Towards Rational Design of Gold(III) Complexes for High-Performance Organic Light-Emitting Devices. *Nature Photon.* **2019**, *13*, 185.
- (56) For further information, see Supporting Information.
- (57) Lauerhaas, J. M.; Credo, G. M.; Heinrich, J. L.; Sailor, M. J. Reversible Luminescence Quenching of Porous Silicon by Solvents. *J. Am. Chem. Soc.* **1992**, *114*, 1911.
- (58) Lee, J.; Chen, H.-F.; Batagoda, T.; Coburn, C.; Djurovich, P. I.; Thompson, M. E.; Forrest, S. R. Deep Blue Phosphorescent Organic Light-Emitting Diodes with Very High Brightness and Efficiency. *Nature Mater.* **2015**, *15*, 92.
- (59) Zhou, D.; To, W.-P.; Kwak, Y.; Cho, Y.; Cheng, G.; Glenna, S. M. T.; Che, C. M. Thermally Stable Donor-Acceptor Type (Alkynyl)Gold(III) TADF Emitters Achieved EQEs and Luminance of upto 23.4% and 70300 cd m<sup>-2</sup> in Vacuum-Deposited OLEDs. *Adv. Sci.* **2019**, *6*, 1802297.
- (60) Chan, K. T.; Tong, G. S. M.; To, W.-P.; Yang, C.; Du, L.; Philips, D. L.; Che, C.-M. The Interplay Between Fluorescence and Phosphorescence with Luminescent Gold(I) and Gold(III) Complexes Bearing Heterocyclic Arylacetylidate Ligands. *Chem. Sci.* **2017**, *8*, 2352.
- (61) Jou, J.-H.; Kumar, S.; Fang, P.-H.; Venkateswararao, A.; Thomas, K. R. J.; Shyue, J.-J.; Wang, Y.-C.; Li, T.-H.; Yu, H.-H., Highly Efficient Ultra-Deep Blue Organic Light-Emitting Diodes with a Wet- and Dry-Process Feasible Cyanofluorene Acetylene Based Emitter. *J. Mater. Chem. C* **2015**, *3*, 2182.
- (62) Kukhta, N. A.; Volyniuk, D.; Grazulevicius, J. V.; Sini, G. Blue Versus Yellow Emission in Bipolar Fluorenone Derivatives: the Impact of Aggregation and Hydrogen Bonding. *J. Mater. Chem. C* **2018**, *6*, 1679.
- (63) Jou, J.-H.; Kumar, S.; Agrawal, A.; Li, T.-H.; Sahoo, S. Approaches for Fabricating High Efficiency Organic Light Emitting Diodes. *J. Mater. Chem. C* **2015**, *3*, 2974.

